A model-based approach to the Common-Diffraction-Surface Stack

Hashem Shahsavani[1], Jürgen Mann[2], Iradj Piruz[1], Peter Hubral[2]

1-Shahrood University of Technology, Shahrood, Iran
2-Karlsruhe Institute of Technology, Karlsruhe, Germany

Summary

❖ The Common-Reflection-Surface stack method parameterizes and stacks seismic reflection events in a generalized stacking velocity analysis. It considers a discrete number of events contributing to a given stack sample such that conflicting dip situations can be handled. The reliable detection of such situations is difficult and missed contributions to the stacked section deteriorate the results of a subsequent migration.

❖ As an alternative, the conflicting dip problem has been addressed by explicitly considering a virtually continuous range of dips with a simplified stacking operator in a process termed Common-Diffraction-Surface stack. The Common-Diffraction-Surface stack has been successfully applied in a data-driven manner based on coherence analysis in the prestack data, i. e., in the same manner as the Common-Reflection-Surface stack. However, in view of the computational costs, the data-driven Common-Diffraction-Surface stack method is very expensive.

❖ We present a much more efficient model-based approach to the Common-Diffraction-Surface stack. This approach only requires a smooth macro-velocity model of minor accuracy. Compared to the data-driven Common-Diffraction-Surface stack approach, the computational effort is dramatically reduced with even improved results. After a subsequent poststack depth migration, the results are very close to the results of a prestack depth migration, without introducing the demands in model accuracy inherent to prestack depth migration.

Introduction

The Common-Reflection-Surface (CRS) stack method follows the concept of the classical stacking velocity analysis, the local parameterization and stacking of reflection events by means of an analytic second-order approximation of the reflection traveltime (see, e. g., Mann et al., 1999). In its simplest implementation, the CRS stack determines only one optimum stacking operator for each zero-offset (ZO) sample to be simulated. Along this operator, we obtain the maximum coherence in the seismic reflection data.

In the presence of curved reflectors or diffractors, various events might intersect each other and/or themselves, such that a single stacking operator per ZO sample is no longer appropriate. To address this,

➤ Mann (2001) proposed to allow for a small, discrete number of stacking operators for a particular ZO sample. The main difficulty in this approach is to identify conflicting dip situations and to decide how many contributions should be considered.

➤ Soleimani et al. (2009a) proposed an adapted CRS strategy by merging concepts of the dip moveout correction with the CRS approach. To simplify this process and to emphasize diffraction events, this has been implemented with a CRS operator reduced to (hypothetical) diffraction events, yielding the so-called Common-Diffraction-Surface (CDS) stack. This **data-driven** CDS stack has been successfully applied to complex land data (Soleimani et al., 2010). However, the data-driven CDS stack is quite time consuming, as separate stacking operators have to be determined for each stacked sample to be simulated.

❖ Here, we propose a **model-based** approach to the CDS stack. We assume that a smooth macro-velocity model has already been determined in which the parameters of the CDS stacking operators can be easily forward-modeled by means of kinematic and dynamic ray tracing such that their determination by means of coherence analysis in the prestack is no longer required. In this way, a complete stacked section optimized for poststack depth migration can be generated in a much more efficient manner compared to the data-driven CDS approach.

Traveltime approximation

The CRS method is based on an analytical approximation of the reflection traveltime up to second order in terms of the half source/receiver offset h and the displacement Δx_m of the source/receiver midpoint x_m with respect to the location x_0 of the stacked trace to be simulated. For the 2D case the hyperbolic CRS traveltime approximation can be expressed as

$$t^2(\Delta x_m, \Delta h) = \left[t_0 + 2\frac{\sin\alpha}{v_0}\Delta x_m\right]^2 + 2t_0\frac{\cos^2\alpha}{v_0}\left(\frac{\Delta x_m^2}{R_N} + \frac{h^2}{R_{NIP}}\right), \quad (1)$$

with v_0 denoting the near-surface velocity. The stacking parameter a is the emergence angle of the normal ray, whereas R_N and R_{NIP} are the local radii of hypothetical wavefronts excited by an exploding reflector experiment or an exploding point source at the (unknown) reflection point of the normal ray, the normal incidence point (NIP). All these properties are defined at the acquisition surface (x_0; z = 0).

For a true diffractor in the subsurface, an exploding point source experiment and an exploding reflector experiment naturally coincide such that $R_{NIP} \equiv R_N$. Thus, for diffraction events, the CRS traveltime equation (1) reduces to the CDS traveltime approximation

$$t^2(\Delta x_m, \Delta h) = \left[t_0 + 2\frac{\sin\alpha}{v_0}\Delta x_m\right]^2 + 2t_0\frac{\cos^2\alpha}{R_{CDS}v_0}(\Delta x_m^2 + h^2), \quad (2)$$

with $R_{CDS} \equiv R_{NIP} \equiv R_N$. For reflection events, the CDS operator (2) is an inferior approximation compared to the full CRS operator (1) as $R_{NIP} \neq R_N$. Nevertheless, it still allows to approximate the event within a

reasonably chosen aperture. For the data-driven CDS stack, this simplified operator has been chosen for performance reasons. For the model-based CDS stack, this simplification is mandatory, as there is no structural information on reflector curvatures contained in the considered smooth macrovelocity model. Thus, a forward-modeling of the lacking parameter R_N is not possible anyway. Note that in the data-driven CDS stack, R_{CDS} represents a weighted average of R_N and R_{NIP}, whereas $R_{CDS} \equiv R_{NIP}$ in the model-based approach presented here. The difference between both definitions is significant!

Forward-modeling

The radius of the NIP wave occurring in the CDS operator (2) is associated with a hypothetical point source at the NIP. The local curvature of the corresponding wavefront is considered along the normal ray. Thus, the first step is to determine the potential normal ray by means of kinematic ray tracing. As we need this ray for a given surface location and a given emergence angle, the kinematic ray tracing is performed for the down-going ray. The corresponding kinematic ray tracing system, in 2D a system of four coupled ordinary differential equations of first order, can be numerically integrated with the well known Runge-Kutta scheme of fourth order. In this way, we directly obtain discrete points along the ray paths corresponding to the desired output locations in the ZO time domain.

The determination of R_{NIP} requires dynamic ray tracing along the ray path. The 2D dynamic ray tracing system consists of two coupled ordinary differential equations of first order. For a given initial condition at a point of the ray, it allows to calculate the second partial derivative of traveltime normal to the ray for any point along the ray. For a point source initial condition at a NIP on the ray, this traveltime derivative is directly related to the searched-for stacking parameter.

Implementation aspects

In addition to the stacked section, the CRS method provides sections with the maximum encountered coherence along the optimum CRS operators and their corresponding sets of wavefield attributes. In the model-based CDS approach we can also obtain similar sections with little additional effort. With the calculated coherence value, we can keep track of the CDS operator yielding the highest coherence for a particular ZO sample.

In the data-driven stack approaches, the size of the search and stacking aperture in midpoint direction is often based on the size of the projected first Fresnel zone. Furthermore, the aperture size has to be kept constant for a particular ZO sample as coherence measures are sensitive to the number of contributing traces which might deteriorate the coherence analysis (see, e. g., Mann, 2002). In the model-based approach, coherence analysis is not employed, such that there is no need for a fixed aperture. In addition, the aperture size in midpoint direction has to be chosen smaller, as the CDS approximation with $R_{CDS} \equiv R_{NIP}$ quickly deviates from the actual event in case of a reflection event. Therefore, we propose to use a smaller aperture centered around the so-called Common-Reflection-Point (CRP) trajectory, where CRS operator and CDS operator are both tangent to the actual event.

Synthetic example: Sigsbee 2A data

To allow for a direct comparison with the data-driven CDS results by Soleimani et al. (2009a) we applied the model-based CDS approach to the well-known synthetic Sigsbee 2A data set (Pfaffenholz, 2001). This data set has been simulated by the SMAART JV by acoustic finite-difference modeling for the stratigraphic model shown in Figure 1. Due to an absorbing top surface, the data contain no free-surface multiples. The data consist of a total of 500 shot gathers with 150 ft shot interval and up to 348 receivers with a spacing of 75 ft. Temporal sampling rate is 8 ms, offsets range from 0 to 26025 ft.
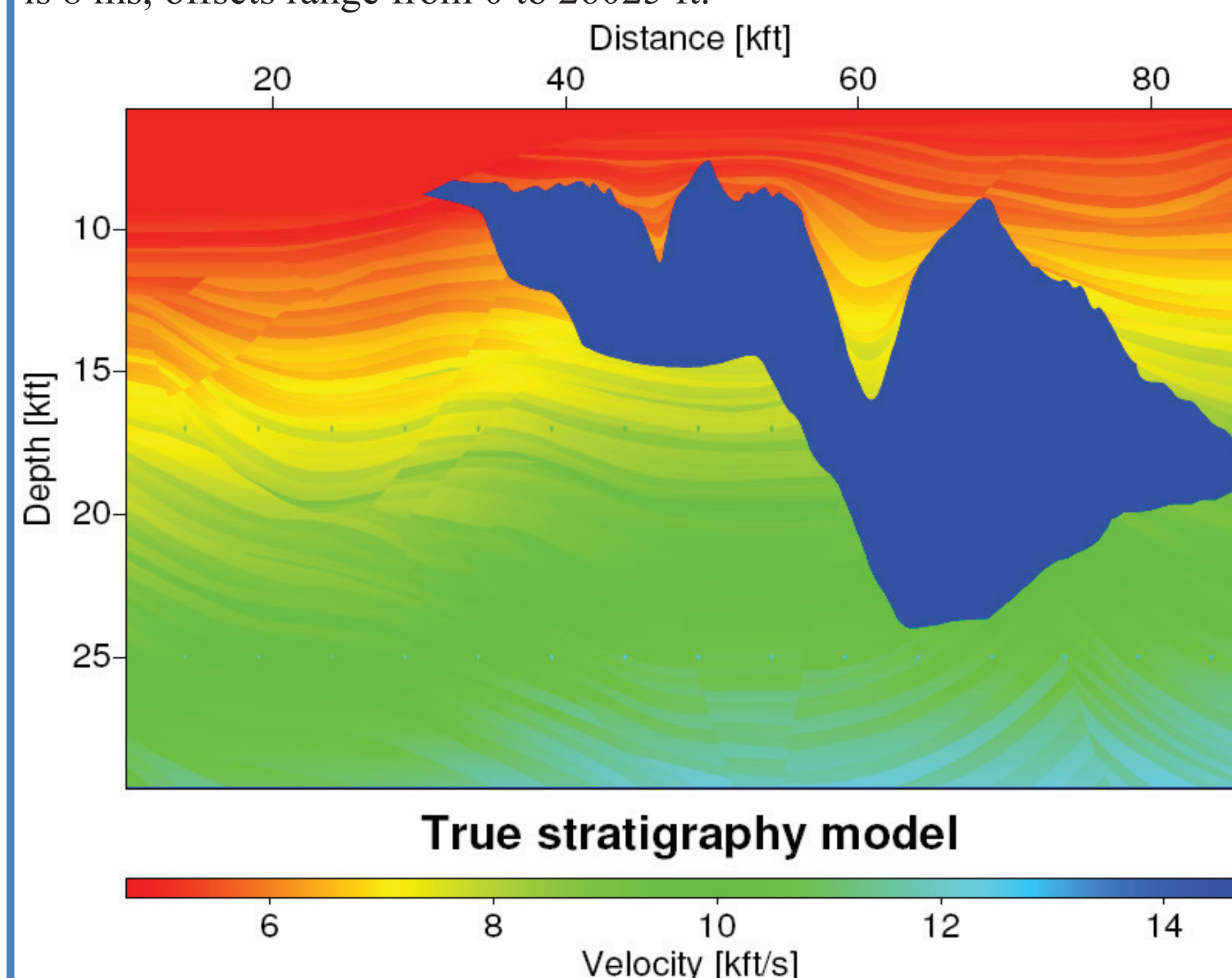

Figure 1: Stratigraphic model used for the simulation of the Sigsbee 2A data.

As we want to focus on the stacking procedure rather than on the generation of the macro-velocity model by means of an inversion, we used the migration velocity model (not shown) distributed with the data as basis for our macro-velocity model.

The migration velocity model consists of the water column, the salt body, and a smooth background velocity, namely a constant vertical gradient of 0.3/s starting with 5000 ft/s at the seafloor. To obtain our macro-model, we first restored the seafloor at those locations where the salt body is in direct contact with the water column and then replaced the salt body by the background gradient. Finally, we smoothed the inverse of the velocity model five times with the auto-convolution of a rectangular box of 525×525 ft[2] to get rid of the sharp velocity contrast at the seafloor without impairing the kinematics of the model.

The kinematic and dynamic ray tracing has been performed for each CMP bin, i. e., with a lateral spacing of 37.5 ft and a temporal step length of 0.8 ms. We did not allow turning rays, although this is supported by the implementation. Rays have been shot for an angle range of ±50° at 2° spacing. For the actual stacking process, the stacking parameter R_{CDS} is linearly interpolated in between the rays on a grid with 1° spacing.

The midpoint aperture has a constant half-width of 300 ft centered around the approximate CRP trajectory (15), the offset aperture ranges from 6000 ft at 2.3 s to 25000 ft at 11 s ZO traveltime. Semblance has been calculated within a time window of 56 ms. The stacked section shown in Figure 2 is very similar to the corresponding result obtained with its data-driven counterpart presented by Soleimani et al. (2009a) (not shown). The latter contains some spurious events which do not show up in the model-based result, but the main difference is the computational cost which is now more than two orders of magnitude lower for this data set (not including the fact that the data-driven result excludes the subsalt region for performance reasons). Of course, with the inherent second-order approximation of the CRS and CDS approaches, we cannot expect any reasonable result for the subsalt region, that is why we have removed the salt body in the macro-velocity model.

The benefits of the complete handling of conflicting dip situations are best seen after a subsequent poststack migration using the macro-velocity model depicted in Figure 1: Figure 3 shows the result of a poststack Kirchhoff depth migration obtained for the model-based stack section shown in Figure 2. All faults and diffractors are well imaged, everything left and above of the salt is well imaged. For comparison, we first revisited the CRS results by Mann (2002). They have been computed with two strategies: the simple approach considering only one dip per ZO sample and the extended approach with up to three dips per ZO sample.
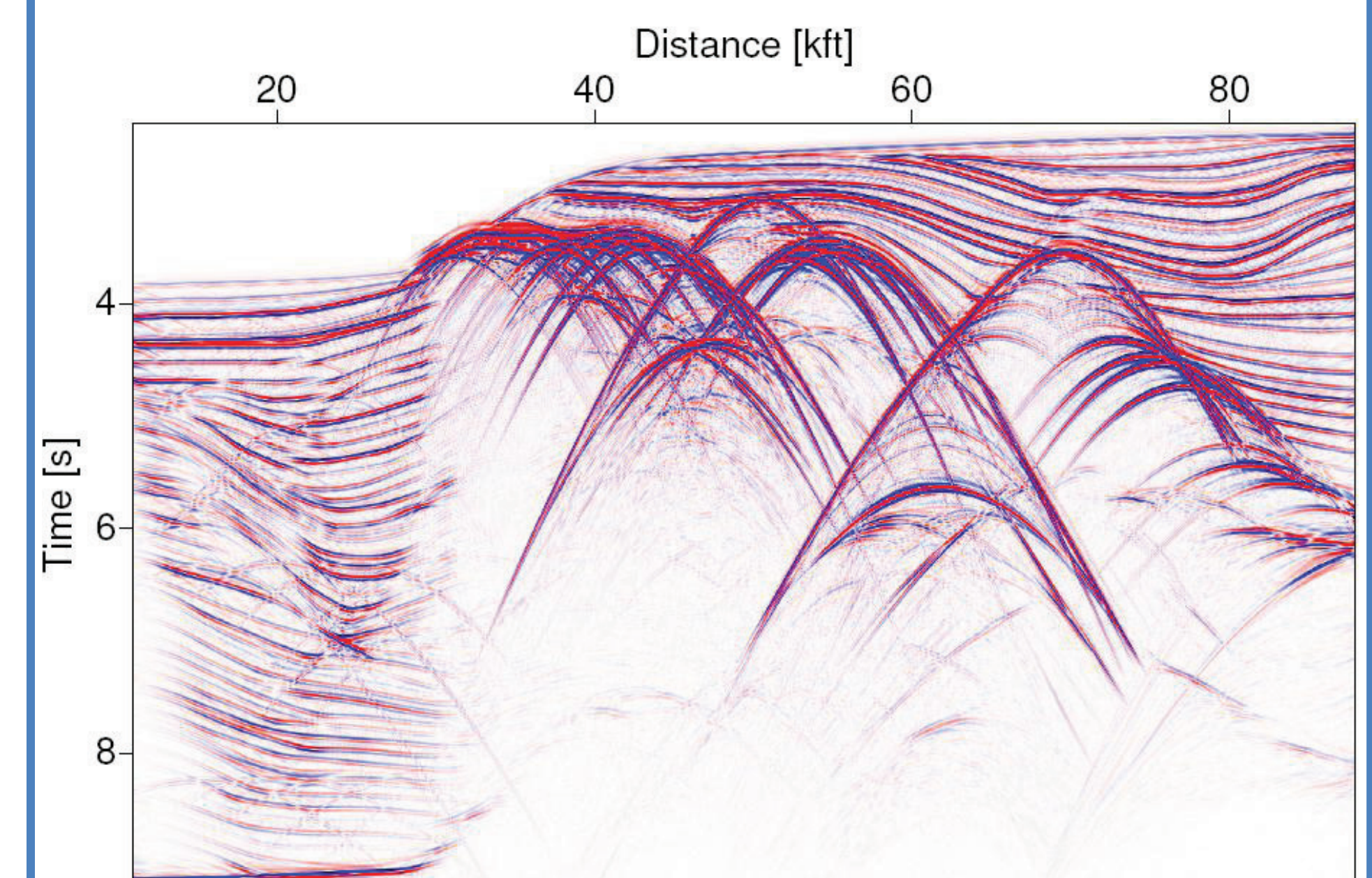

Model-based CDS stack section

Figure 2: Stacked section obtained with the model-based CDS approach. Note the various diffraction patterns caused by true diffractors, wedges, and model discretization.
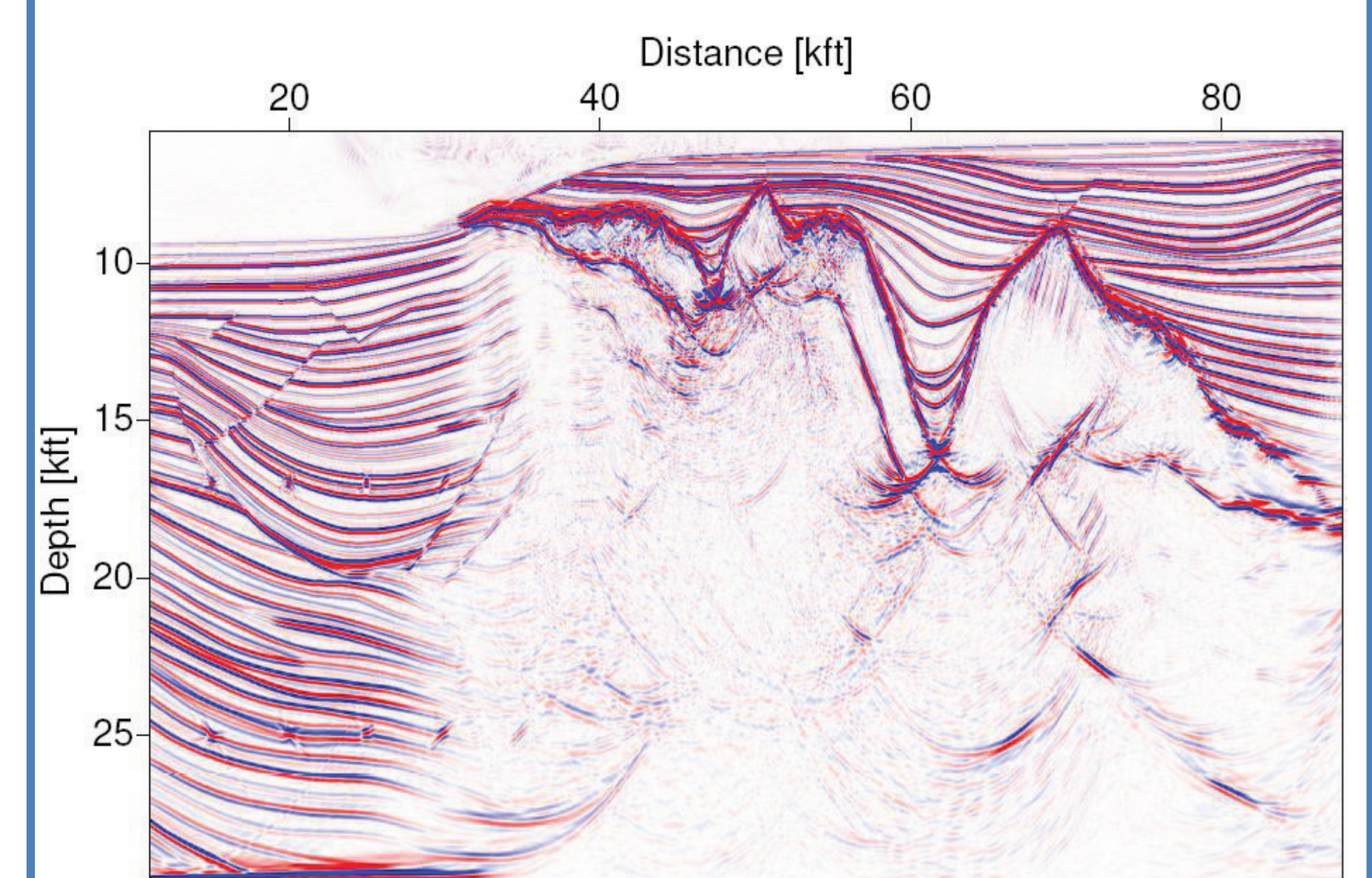
PostSDM of model-based CDS stack

Figure 3: Poststack Kirchhoff depth migration result for the model-based stack section shown in Figure 2. Faults and diffractors are clearly focused.
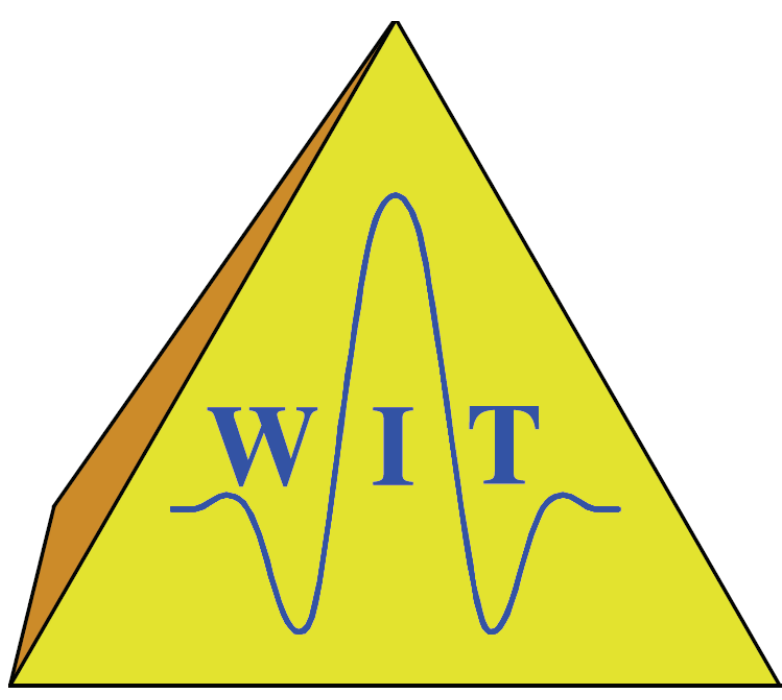
Wave Inversion Technology

Shahrood University Of Technology

Karlsruhe Institute of Technology

Vienna |'11

A model-based approach to the Common-Diffraction-Surface Stack

Hashem Shahsavani[1], Jürgen Mann[2], Iradj Piruz[1], Peter Hubral[2]

1-Shahrood University of Technology, Shahrood, Iran
2-Karlsruhe Institute of Technology, Karlsruhe, Germany

The poststack migration of the latter is depicted in Figure 4. Faults and diffractors are only partly focused. Spurious events in the stacked section, e. g. associated with a change of the number of contributions from sample to sample, cause various artifacts showing up as isochrones in the migrated section.
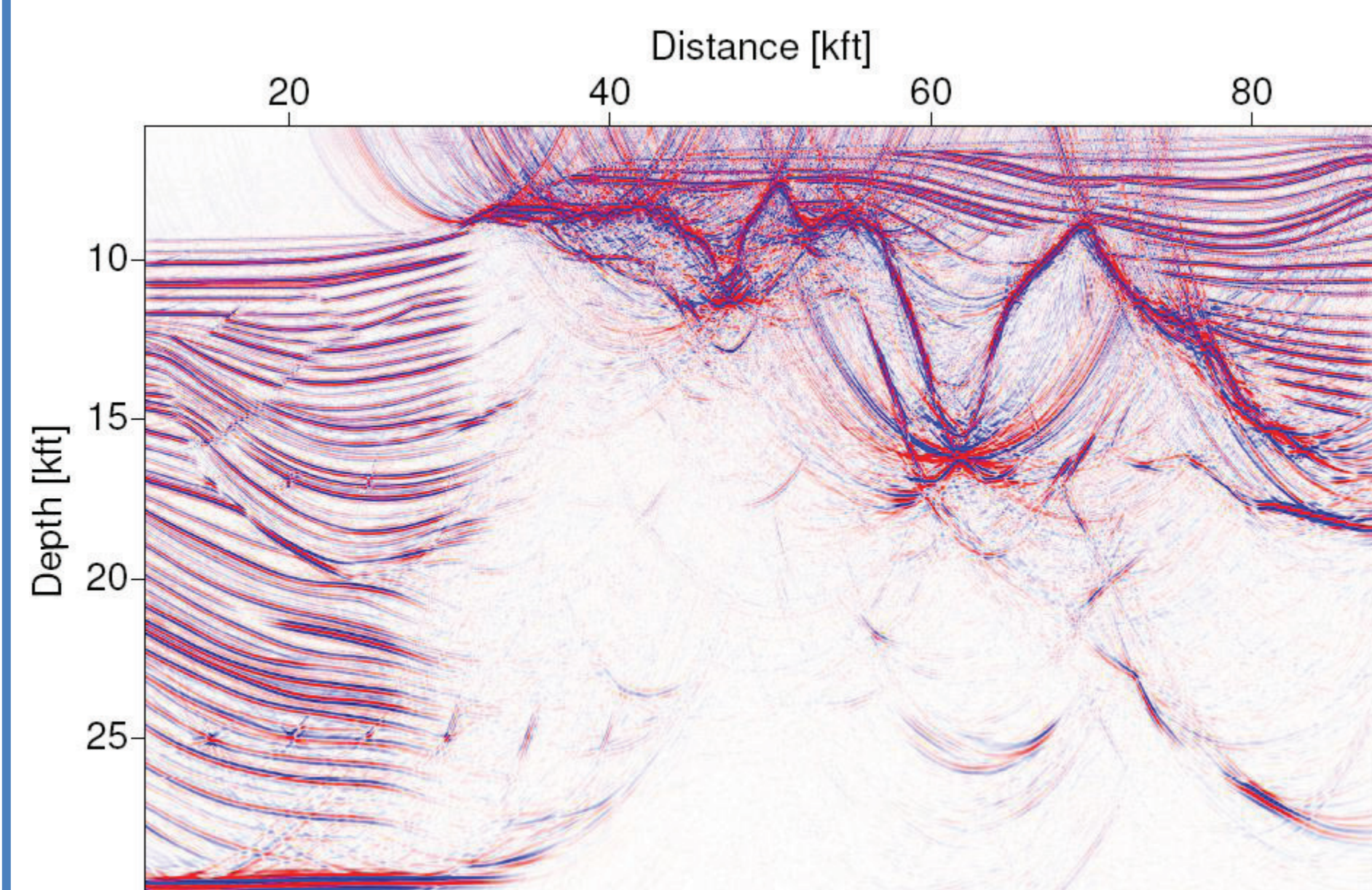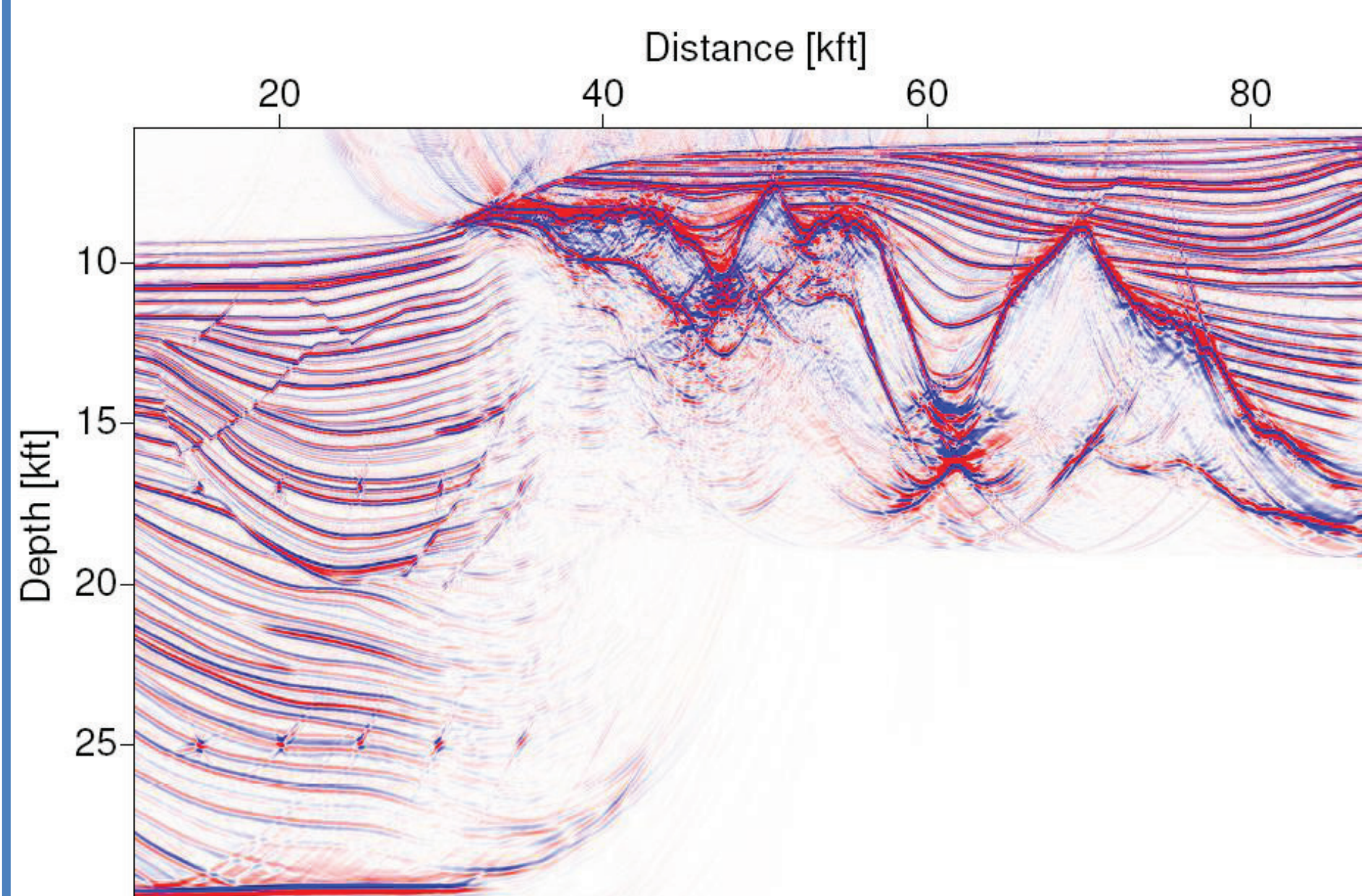

PostSDM of CRS stack

Figure 4: Poststack Kirchhoff depth migration result for the CRS stack result published by Mann (2002). Up to three dips have been considered for each ZO sample. Faults and diffractors are only partly focused, many isochrones caused by spurious events can be seen.

The result based on the CRS stack with only one dip (not displayed) differs from the multi-dip CRS-stacked section in two respects: on the one hand, due to the lacking contributions at conflicting dip locations, the diffractors and faults appear even less focused and with lower amplitudes. On the other hand, the stacked section contains less spurious events such that we have less artifacts in the migrated section. In both cases, the results of poststack migration are unsatisfactory.

The synclines in the top salt are incomplete and accompanied by coherent artifacts at slightly larger depths. As discussed by Mann (2002), the CRS stack has most likely also parameterized and stacked events associated with prismatic waves which lead to additional events in the stacked section. CRS for ZO simulation as well as poststack migration both imply normal rays, such that prismatic waves cannot be correctly imaged. Note that this effect hardly occurs in the model-based result shown in Figure 3: As we explicitly forward-model normal rays there, the events from prismatic waves are attenuated by destructive interference.


PostSDM of data-driven CDS stack

Figure 5: Poststack Kirchhoff depth migration result for the data-driven CDS result published by Soleimani et al. (2009a). Faults and diffractors are well focused, there are only few isochrones caused by spurious events.

For the next comparison, we revisited the data-driven CDS results by Soleimani et al. (2009a). The corresponding poststack-migrated section displayed in Figure 5 shows well focused diffractors and faults and much less artifacts caused by spurious events compared to the CRS-based result in Figure 4. As in the CRS-based result, the synclines in the top salt are still not properly imaged, as the data-driven CDS stack picks up prismatic waves as well.

As a final reference, we also applied a Kirchhoff prestack depth migration to the prestack data using the same macro-velocity model. The offset range and the muting of the migrated images gather were chosen such that they match the corresponding parameters used during the CDS stack as closely as possible. Figure 6 shows the stack of about 80 offset bins with a width of 300 ft after depth-dependent muting. The prismatic waves are again imaged wrongly, but cancel out during the stack. This section is very similar to the poststack migration of the model-based CDS-stacked section in Figure 2.
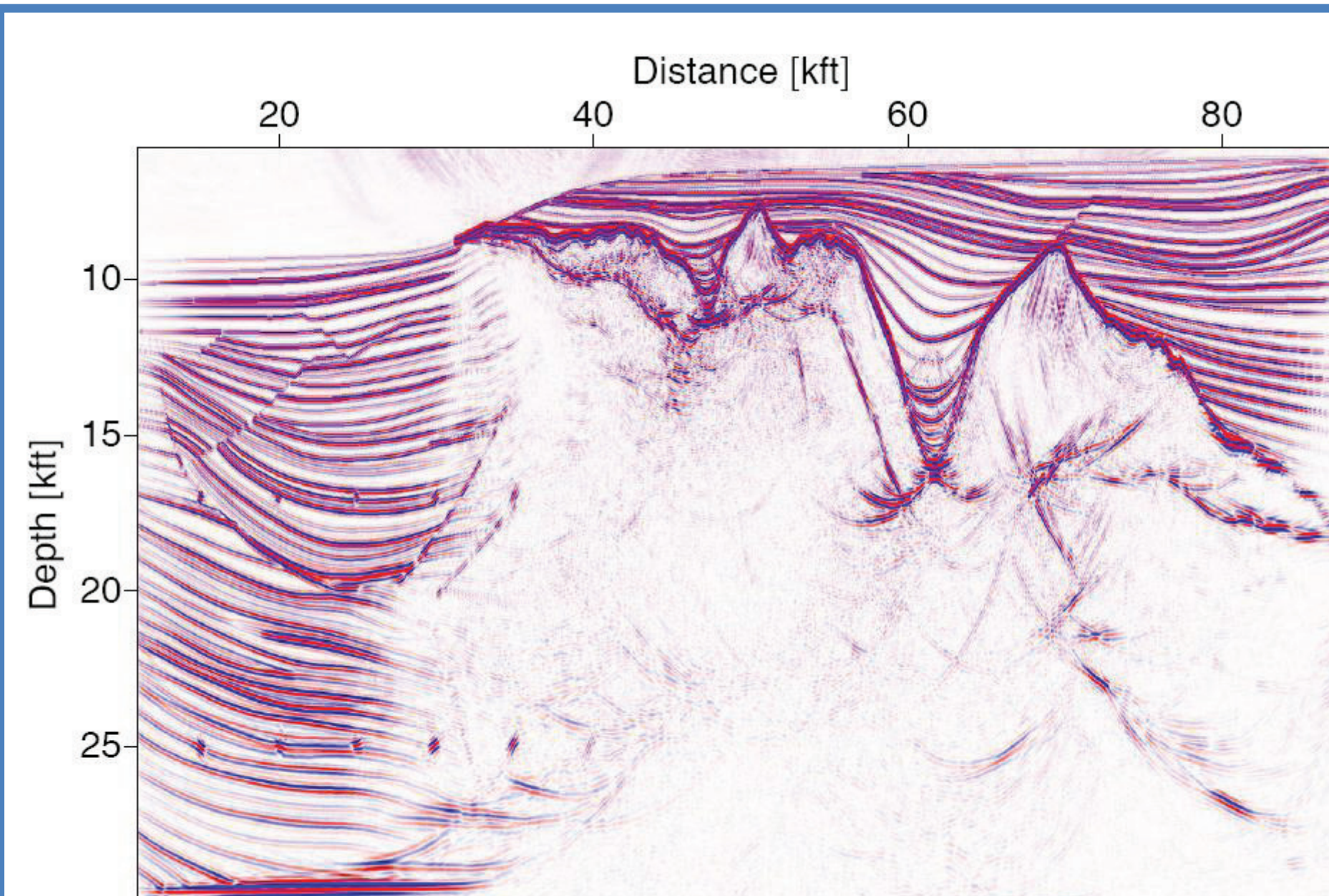
Prestack depth migration

Figure 6: Prestack Kirchhoff depth migration result with high similarity to the poststack result shown in Figure 3. To allow for a fair comparison, the used offset range coincides with the one used for the CDS stack and the image gathers have been muted such that they mimic the time-dependent CDS stacking aperture in offset direction.

As mentioned above, we can perform coherence analysis along the individual forward-calculated stacking operators in the prestack data with little additional effort. As an example, the section with the highest coherence values encountered for each individual ZO sample is depicted Figure 7. It allows to identify the reflection events and to evaluate the local fit between CDS operator and event.
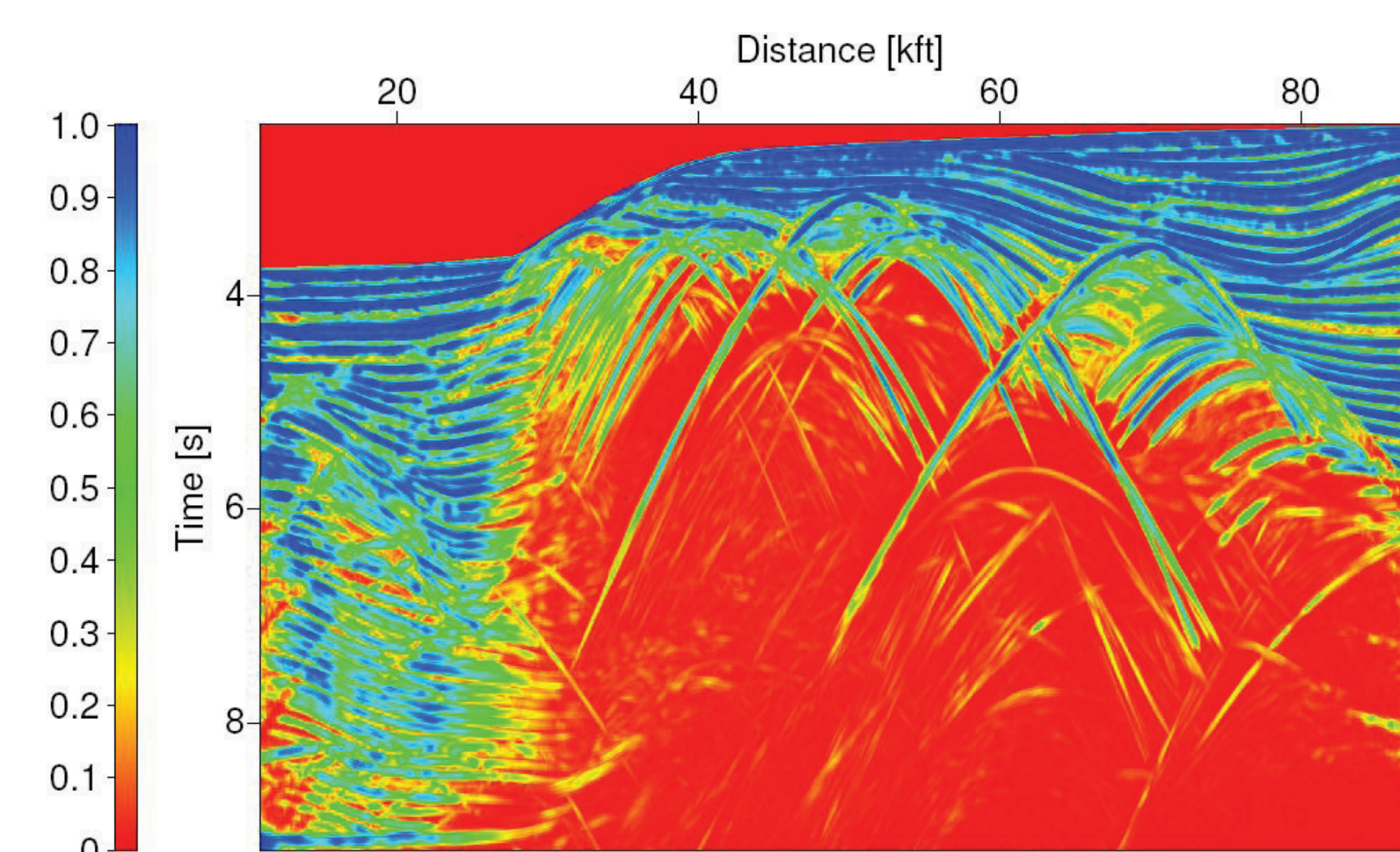

Coherence along dominant events

Figure 7: Section of maximum encountered semblance corresponding to the stack section shown in Figure 2. The associated attribute pairs (α, R_{NIP}) form attribute sections (not shown) resembling the analogous sections of the CRS approach.

Together with the coherence along the most prominent operator, we can also store the corresponding stacking parameters α and R_{CDS} for each ZO sample. For inversion the attributes of the model-based CDS stack are obviously of no use, because they are forward calculated. Inverting for them will, thus, at best reproduce the macro-velocity model already employed for stacking.

Figure 8 shows the result of an attribute-based time migration using the forward-modeled attributes. Although there are various artifacts in this section, the sedimentary part looks quite reasonable. Note that CRS-based counterpart (not shown) presented by Mann (2002) strongly suffers from high frequency noise and huge gaps in the events due to missing or unstable attributes.
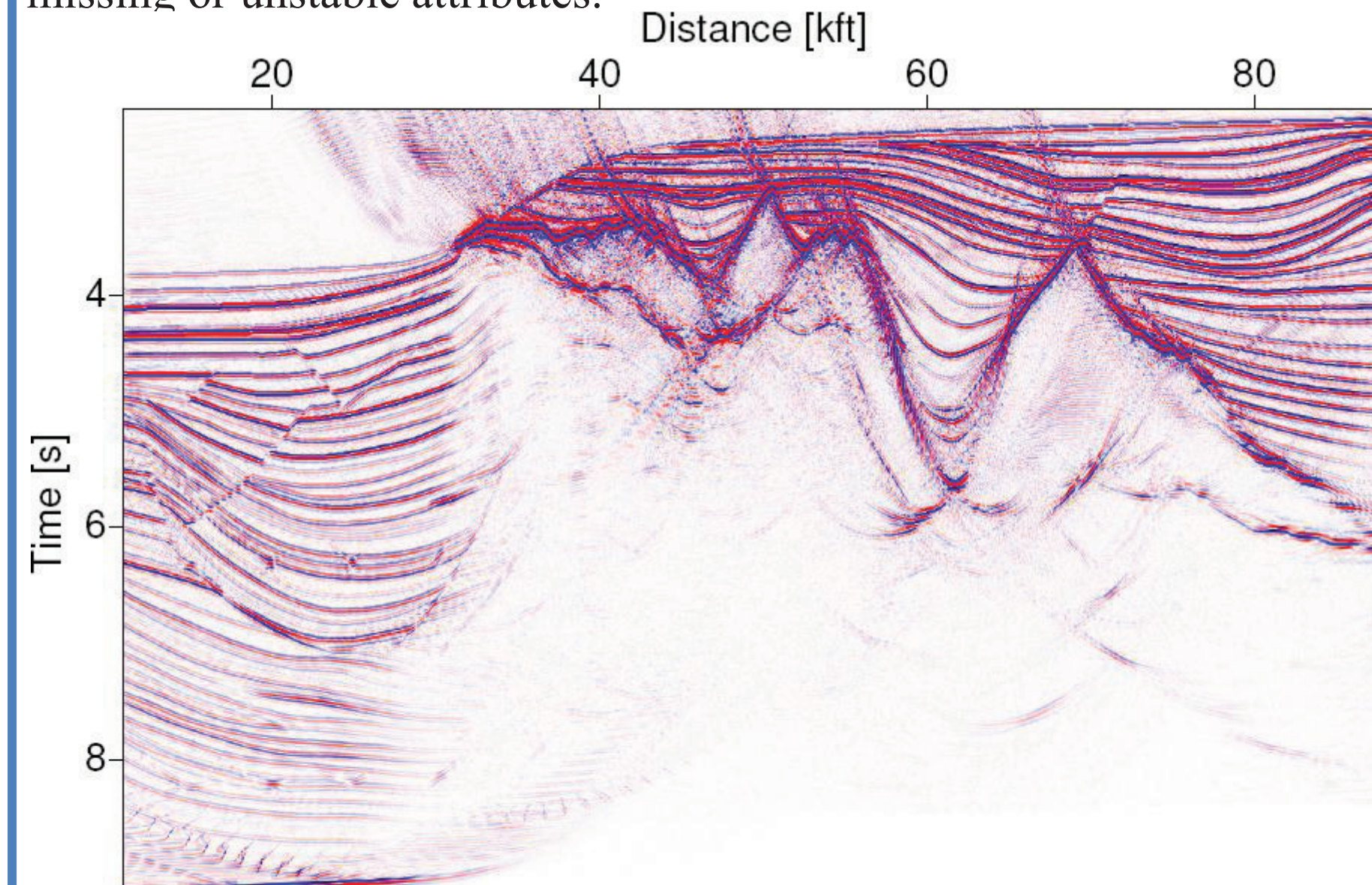
Pseudo time migrated CDS stack section

Figure 8: Attribute-based time migration result obtained as a by-product of the model-based CDS stack. Compared to the CRS-based counterpart (not shown), more stable attributes and the quasi-continuous range of contributing emergence angles render this very simple approach feasible for the sedimentary regions

Conclusions and outlook

We have implemented and applied a model-based approach to the CDS stack method. This method is intended to fully resolve the conflicting dip problem occurring in complex data and, thus, to allow to simulate a complete stacked section containing all mutually interfering reflection and/or diffraction events. In contrast to the entirely data-driven CDS method (Soleimani et al., 2009b,a), this model-based approach is far more efficient. The required macro-velocity model can be generated with any inversion method, including the sequential application of CRS stack and NIP-wave tomography. For the Sigsbee 2A data presented here, we excluded the inversion aspect and used a simplified version of the migration velocity model distributed with the data. The model-based CDS stack is tailored to optimize the stacked section for a subsequent poststack depth migration. This is relevant for situations in which the generation of velocity models sufficiently accurate for prestack depth migration is difficult or even impossible. For the Sigsbee 2A data, we demonstrated that the model-based CDS stack allows to generate a poststack-migrated section very similar to the corresponding prestack migration result. The latter process usually requires a more accurate macro-velocity model. The new approach yields even better results than the data-driven approach in a significantly shorter computation time. The model-based CDS stack can be integrated into the CRS-based imaging workflow in situations where the result of NIP wave tomography might not be sufficiently accurate to perform a prestack depth migration: as schematically shown in Figure 9 prestack migration might be replaced by a sequence of model-based CDS stack and poststack migration. In this way, we can overcome the former deficiencies of the CRS stack section which lead to gaps and artifacts in the poststack migration result.
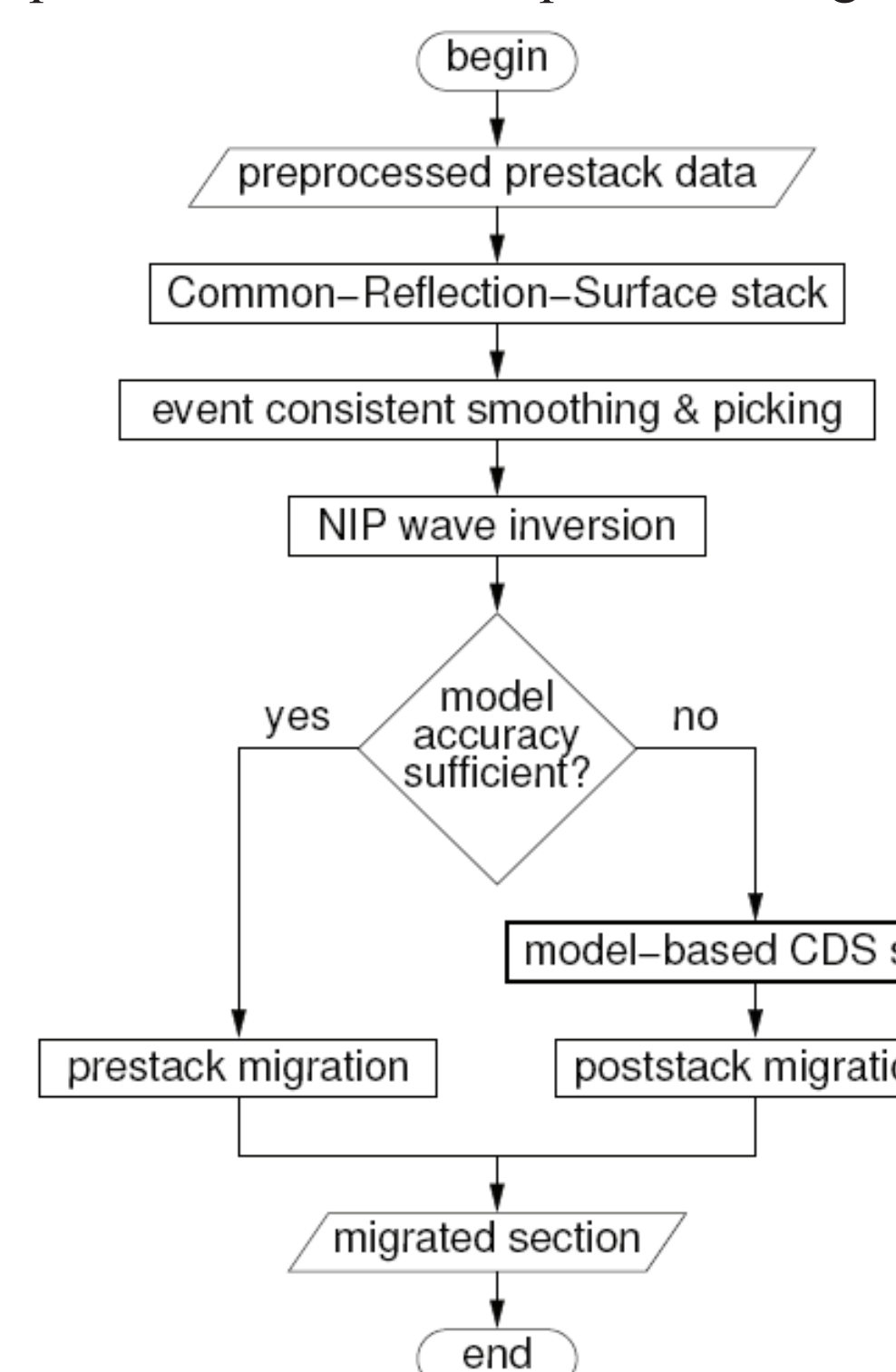

Figure 9: Processing flowchart with an alternative to prestack migration using the model-based CDS stack plus poststack depth migration.

References

Mann, J., Jäger, R., Müller, T., Höcht, G., and Hubral, P. (1999). Common-Reflection- Surface stack – a real data example. J. Appl. Geophys., 42(3,4):301–318.

Mann, J., Hubral, P., Traub, B., Gerst, A., and Meyer, H. (2000). Macro-model independent approximative prestack time migration. In Extended abstracts, 62nd Conf. Eur. Assn. Geosci. Eng., B-52.

Mann, J. (2001). Common-Reflection-Surface stack and conflicting dips. Extended abstracts, 63rd Conf. Eur. Assn. Geosci. Eng., P077.

Mann, J. (2002). Extensions and applications of the Common-Reflection-Surface Stack method. Logos Verlag, Berlin.

Pfaffenholz, J. (2001). Sigsbee2 synthetic subsalt data set: image quality as function of migration algorithm and velocity model error. In Workshop on velocity model independent imaging for complex media, Extended abstracts. Soc. Expl. Geophys., W5-5.

Soleimani, M., Piruz, I., Mann, J., and Hubral, P. (2009a). Common Reflection-Surface stack: accounting for conflicting dip situations by considering all possible dips. J. Seis. Expl., 18(3):271–288.

Soleimani, M., Piruz, I., Mann, J., and Hubral, P. (2009b). Solving the problem of conflicting dips in Common-Reflection-Surface stack. In Extended Abstracts, 1st Internat. Conf. & Exhib., Shiraz, Iran. Eur. Assn. Geosci. Eng.

Soleimani, M., Mann, J., Adibi Sedeh, E., and Piruz, I. (2010). Improving the seismic image quality in semi-complex structures in North East Iran by the CDS stack method. In Extended abstracts, 72nd Conf. Eur. Assn. Geosci. Eng., P398.